

Lung Image Segmentation using Rotation Invariance and Template Matching

Nidhi, Varun Bhardwaj

Abstract— The work aims at using the rotation invariant feature and gray scale invariance feature as basis for template matching for identification of nodules of various sizes and texture. The structural textures so obtained are used to describe statistical feature called variance which provide efficient segmentation of lung nodules and helps in clear visualization of nodule boundaries which is important for doctors for analyzing the disease effects. The segmented image so obtained showed all the nodules clearly but the nodules that benign cannot be separated or identified by segmentation. To identify the nodule so obtained the different size templates of nodules were described to identify nodules of particular size and texture. The LBP variance descriptor provided the texture and LBP rotation invariance allowed nodule to be detected irrespective of the orientation of input image.

Keywords- LBP.

I. INTRODUCTION

SO far many methods have been devised for detection of lung cancer. The concept of rotation invariant linear binary pattern has not been used in combination with template matching for detection of nodules in lung images. The only paper published in this context is in June 2011.

The research has been started in this context and more people are trying to develop an efficient method for lung nodule detection due to high robustness of the LBP method and characteristics like rotation and scale invariance. The process comprise of following step each of which is described in detail in next section:

- 1) Data Acquisition
- 2) Feature Extraction
- 3) Data Conversion
- 4) Lung Segmentation
- 5) Segmentation of nodule
 - a. Uniform Linear Binary Patterns
 - b. Rotation invariant Binary patterns
 - c. Uniform Linear Binary Variance Operator
 - d. Rotation invariant Linear Binary pattern Variance Operator
- 6) Template Matching
 - a. Parenchymal nodule (15mm,18mm,20mm)
 - b. Juxtapleural nodule (15 mm)
- 7) Evaluation
 - a. Sensitivity and Specificity
 - b. Accuracy

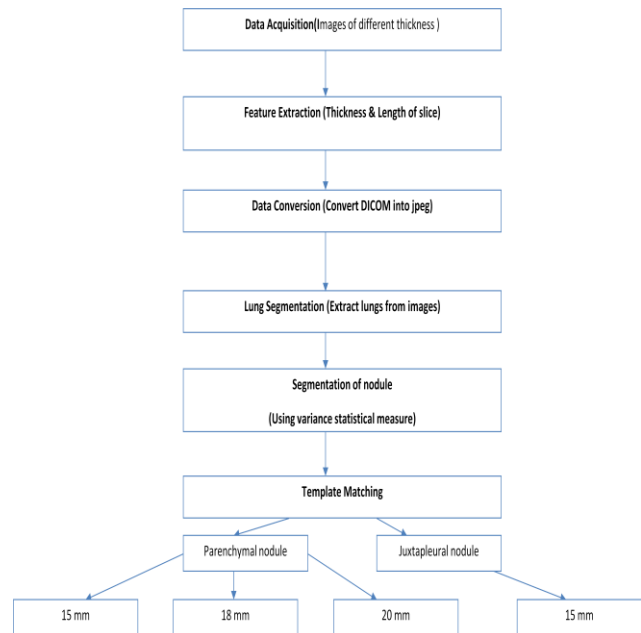


Fig 1: Flowchart of Complete Process

II. DATA ACQUISITION AND FEATURE EXTRACTION

For the purpose of the present work, Database of lung images of was downloaded from Lung Image Database Consortium [1], it is a publicly available. The database so obtained contains DICOM data series 1.3.6.1.4.1.9328.50.3.0022 with each series comprising of series of images showing lung at different thickness [2]. The database was divided into groups according to following:
Slice Thickness: 1.3 mm,1.5 mm, 2.0 mm, 2.5 mm ,3.0 mm.

Slice Length: From each set of available thickness, slice length was observed for which the lungs were visible in images as suggested by the Dr Khandelewal form PGI whom we consulted for helping us find the nodule present in images and suggesting how to discriminate it from other false lights present in image. The figure below presents the studied data out of which best values were chosen that covers maximum images with full lung view present in them forming the next table.

Manuscript received January 15, 2014.

Nidhi, Department of Computer Engineering, NIT Kurukshetra,
Varun Bhardwaj Department of Business Intelligence Infosys Technologies



Patient-ID	Slice Thickness (In mm)	Slice Length for false Start images (In mm)	Slice Length for lung start(In mm)	Slice length false end images (In mm)
1.3.6.1.4.1.9328.50.3.0025	1.3	-25.7	-90.7	-163.2
1.3.6.1.4.1.9328.50.3.0026		-5.8	-59.8	-243.5
1.3.6.1.4.1.9328.50.3.0034	1.5	-351.9	-427.6	-478.6
1.3.6.1.4.1.9328.50.3.0041	2.0	-99.6	-128.40	-246
1.3.6.1.4.1.9328.50.3.0042		1022	856	249
1.3.6.1.4.1.9328.50.3.0043		-39	-249.60	-250
1.3.6.1.4.1.9328.50.3.0044		-108.0	-167	-290
1.3.6.1.4.1.9328.50.3.0045		-32	-113	-194
1.3.6.1.4.1.9328.50.3.0046		2.5	13.8	-132
1.3.6.1.4.1.9328.50.3.0047	40.4		-123	-232
1.3.6.1.4.1.9328.50.3.0048	36.2		-101.8	-148.8
1.3.6.1.4.1.9328.50.3.0049	-6.2		-138	-220
1.3.6.1.4.1.9328.50.3.0050	-22.8		-113.2	-169.2
1.3.6.1.4.1.9328.50.3.0031	3.0	1692	1587	1500
1.3.6.1.4.1.9328.50.3.0032		-43.0	-148.0	-226.0
1.3.6.1.4.1.9328.50.3.0033		1647	1515.5	1434.5

Table 1: Database Distribution

III. IMAGE CONVERSION

The DICOM images so obtained are converted in jpeg format using lossless conversion. The images formed using MATLAB were found to be blurred thus the image obtained after conversion is saved as lossless jpg image to retain the quality and information present in image.

IV. LUNG SEGMENTATION

Lung segmentation algorithm for image retrieval

- 1) The image is thresholded to separate low-density tissue (eg. lungs) from fat.
- 2) The surrounding air, identified as low-density tissue, is removed.
- 3) Cleaning is performed to remove noise using imfill().
- 4) Lung mask
- 5) Lung Extraction

1. Optimal Thresholding:

The first step is thresholding the image. A CT contains two main groups of pixels: 1) high-intensity pixels located in the body (body pixels), and 2) low-intensity pixels that are in the lung and the surrounding air (non-body pixels). Due to the large difference in intensity between these two groups, thresholding leads to a good separation. Every pixel with an intensity higher than 80 is set to 0 (body pixels) and the others pixels are set to 1 (non-body pixels).

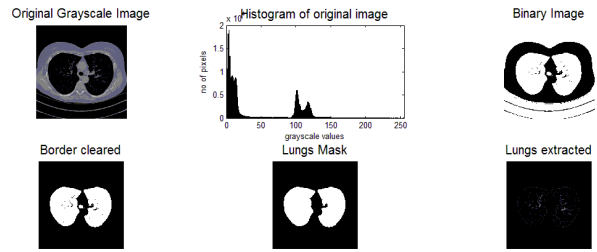


Fig 2: Segmentation steps: (a) Original (b) Thresholding point using histogram (c) Binary Image (d) Noise removal (e) Lung Mask (f) Lungs Extraction

2. Background removal

Background pixels are identified as follow: they are non-body pixels and connected to the borders of the image. Thus, every connected region of non-body pixel that touches the border is considered as background and discarded.

3. Cleaning

Once the background is removed, several non-body regions remain. Holes are present in binary image so formed which are cleared using imfill() function of MATLAB.

4. Lung Mask:

To extract lungs from background lung mask is created. Labeling: Labels are created for all the objects present in image w.r.t to area of object. Sorting: The objects so obtained are sorted according to their size in decreasing order with first two objects being largest in size.

Blob Extraction: The objects obtained after sorting are the Binary Large Objects and represent area covered by lungs. This gives us outline of lungs

5. Lung Extraction:

BLOB's representing lungs are then subtracted from original image to provide lungs for further processing [3].

V. SEGMENTATION OF NODULE

- 1) Uniform Linear Binary Patterns
- 2) Rotation invariant Binary patterns
- 3) Uniform Linear Binary Variance Operator
- 4) Rotation invariant Linear Binary pattern Variance Operator

Local Binary Pattern (LBP) is a simple yet very efficient texture operator which labels the pixels of an image by thresholding the neighborhood of each pixel and considers the result as a binary number[4]. Due to its discriminative power and computational simplicity, LBP texture operator has become a popular approach in various applications

1) Uniform Linear Binary Operator

Uniform patterns can be used to reduce the length of the feature vector and implement a simple rotation-invariant descriptor. Some binary patterns occur more commonly in texture images than others. A local binary pattern is called uniform if the binary pattern contains at most two bitwise transitions from 0 to 1 or vice versa when the bit pattern is traversed circularly.



For example, the patterns 00000000 (0 transitions), 01110000 (2 transitions) and 11001111 (2 transitions) are uniform whereas the patterns 11001001 (4 transitions) and 01010010 (6 transitions) are not

The following notation is used for the LBP operator: LBPP:Ru2. The subscript represents using the operator in a (P:R) neighborhood. Superscript u2 stands for using only uniform patterns and labeling all remaining patterns with a single label. After the LBP labeled image $fl(x,y)$ has been obtained, the LBP histogram can be defined as

$$H_i = \sum_{x,y} I \{f_l(x,y) = i\}, i = 0, \dots, n - 1,$$

Where n is the number of different labels produced by the LBP operator, and $I\{A\}$ is 1 if A is true and 0 if A is false.

2) Rotation Invariant Uniform Binary Operator

The LBPP:R operator produces 2P different output values, corresponding to the 2P different binary patterns that can be formed by the P pixels in the neighbor set. When the image is rotated, the gray values g_p will correspondingly move along the perimeter of the circle around g_0 . Since g_0 is always assigned to be the gray value of element (0: R) to the right of g_c rotating a particular binary pattern naturally results in a different LBPP:R value. This does not apply to patterns comprising of only 0s (or 1s) which remain constant at all rotation angles [5]. To remove the effect of rotation, i.e., to assign a unique identifier to each rotation invariant local binary pattern (ojala et al) defines:

$$LBP_{P,R}^i = \min\{ROR(LBP_{P,R}, i) \mid i = 0, 1, \dots, P - 1\},$$

where ROR. Performs a circular bit-wise right shift on the P-bit number i times.

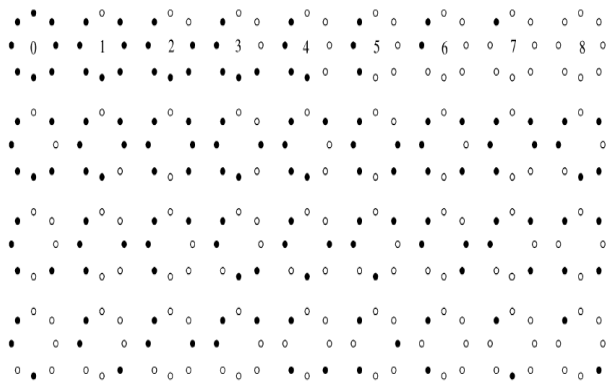


Fig 3: The 36 unique rotation invariant binary patterns that can occur in the circularly symmetric neighbor set of LBPPri8:R. Black and white circles correspond to bit values of 0 and 1 in the 8-bit output of the operator. The first row contains the nine uniform patterns and the numbers inside them correspond to their unique LBPPri2 8:R codes.

3) Uniform Linear Binary Variance Operator and Rotation invariant Linear Binary pattern Variance Operator

Rotation invariant variance measures (VAR).A rotation invariant measure of the local variance can be defined as

$$VAR_{P,R} = \frac{1}{P} \sum_{p=0}^{P-1} (g_p - u)^2$$

where $u = 1/P \sum_{p=0}^{P-1} g_p$.

Since LBPP:R and VARP:R are complementary , their joint distribution LBPP:R =VAR P:R can better characterize the image local texture than using LBPP:R alone. However, LBPu2 P:R is not rotation invariant and it has higher dimensions. In practice, the same (P, R) values are used for LBPPri2P:R and VARP:R. 2.3. LBP variance (LBPV) LBPP:R =VAR P:R is powerful because it exploits the complementary information of local spatial pattern and local contrast [6,7]. However, VARP:R has continuous values and it has to be quantized. This can be done by first calculating feature distributions from all Training images to get a total distribution and then, to guarantee the highest quantization resolution, some threshold values are computed to partition the total distribution into N bins with an equal number of entries. These threshold values are used to quantize the VAR of the test images. There are three particular limitations to this quantization procedure. First, it requires a training stage to determine the threshold value for each bin. Second, because different classes of textures may have very different contrasts, the quantization is dependent on the training samples. Last, there is an important parameter, i.e. the number of bins, to be preset. Too few bins will fail to provide enough discriminative information while too many bins may lead to sparse and unstable histograms and make the feature size too large. Although there are some rules to guide selection [8,9], it is hard to obtain an optimal number of bins in terms of accuracy and feature size. The LBPV descriptor proposed in this section offers a solution to the above problems of LBPP:R=VARP:R descriptor. The LBPV is a simplified but efficient joint LBP and contrast distribution method. As can be seen in equation, calculation of the LBP histogram H does not involve the information of variance VARP;R. That is to say, no matter what the LBP variance of the local region, histogram calculation assigns the same weight 1 to each LBP pattern [10]. Actually, the variance is related to the texture feature. Usually the high frequency texture regions will have higher variances and they contribute more to the discrimination of texture images. Therefore, the variance VARP:R can be used as an adaptive weight to adjust the contribution of the LBP code in histogram calculation

$$LBPV_{P,R}(k) = \sum_{i=1}^N \sum_{j=1}^M w(LBP_{P,R}(i,j), k), k \in [0, K]$$

$$w(LBP_{P,R}(i,j), k) = \begin{cases} VAR_{P,R}(i,j), & LBP_{P,R}(i,j) = k \\ 0 & \text{otherwise} \end{cases}$$

Segmentation is the partitioning of an image into a set of regions with similar visual properties.

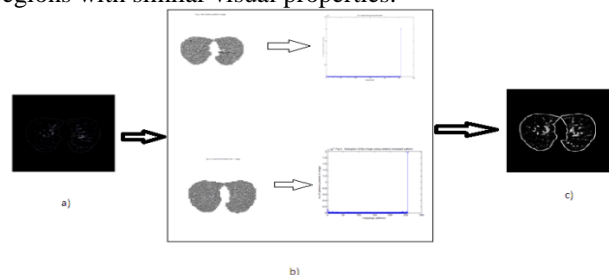


Fig 4: a) Original image b) Feature Extraction Using LBP operators c) Segmented Image



VI. TEMPLATE MATCHING

Template matching is a technique in digital image processing for finding small parts of an image which match a template image. The image and templates are made rotation invariant to have efficient template matching. This method is implemented by first picking out a part of the search image to use as a template: We will call the search image $S(x, y)$, where (x, y) represent the coordinates of each pixel in the search image. We will call the template $T(x t, y t)$, where (xt, yt) represent the coordinates of each pixel in the template. We then simply move the center (or the origin) of the template $T(x t, y t)$ over each (x, y) point in the search image and calculate the sum of products between the coefficients in $S(x, y)$ and $T(xt, yt)$ over the whole area spanned by the template. As all possible positions of the template with respect to the search image are considered, the position with the highest score is the best position [11].

A pixel in the search image with coordinates (xs, ys) has intensity $I_s(xs, ys)$ and a pixel in the template with coordinates (xt, yt) has intensity $I_t(xt, yt)$. Thus the sum of absolute difference in the pixel intensities is defined as $Diff(xs, ys, xt, yt) = |I_s(xs, ys) - I_t(xt, yt)|$.

$$SAD(x, y) = \sum_{i=0}^{T_{rows}} \sum_{j=0}^{T_{cols}} Diff(x+i, y+j, i, j)$$

The mathematical representation of the idea about looping through the pixels in the search image as we translate the origin of the template at every pixel and take the SAD measure is the following:

$$\sum_{x=0}^{S_{rows}} \sum_{y=0}^{S_{cols}} SAD(x, y)$$

S_{rows} and S_{cols} denote the rows and the columns of the search image and T_{rows} and T_{cols} denote the rows and the columns of the template image, respectively. In this method the lowest SAD score gives the estimate for the best position of template within the search image. The method is simple to implement and understand, but it is one of the slowest methods. The templates used are shown below



Fig 5: Template with diameter 10, 15 and 20 mm circular nodules and one juxtalexteral nodule.

Linear binary pattern is computed for both input image and template and feature vector is created for both images. The template however is rotated at 30, 45, 60 and 90 degrees and the feature vector is updated with all rotation angles features also present in it. Thus the template when matched with original image is matched at all the orientations and not just single orientation which provides rotation invariant template matching. Since Linear Binary Pattern converts image in form that patterns are reduced to very small number of patterns only uniform patterns are used while template matching. Red color marking is used to point the matching patterns.

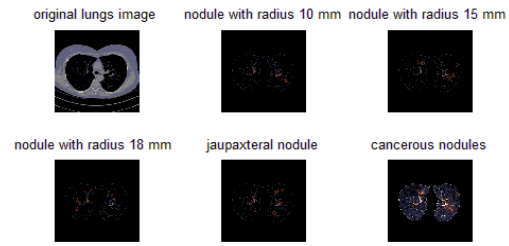


Fig 6: Final output showing marking of corresponding nodules a)original image b) image marked with parenchymal nodules of size 10 mm c) parenchymal nodule with radius 15 mm d) parenchymal nodule with 18 mm radius e) juxtalexteral nodule with radius 18 mm

VII. EVALUATION

Evaluation stages are divided in two parts segmentation evaluation and template matching evaluation. Accuracy is how close a measured value is to the actual (true) value. Precision is how close the measured values are to each other.

Sensitivity

Sensitivity relates to the test's ability to identify positive results. The sensitivity of a test is the proportion of people who have the disease who test positive for it. This can also be written as:

$$\text{sensitivity} = \frac{\text{number of true positives}}{\text{number of true positives} + \text{number of false negatives}}$$

= probability of a positive test given that the patient is ill
If a test has high sensitivity then a negative result would suggest the absence of disease. For example, a sensitivity of 100% means that the test recognizes all actual positives – i.e. all sick people are recognized as being ill. Thus, in contrast to a high specificity test, negative results in a high sensitivity test are used to rule out the disease [12].

Specificity

Specificity relates to the ability of the test to identify negative results.

Consider the example of the medical test used to identify a disease. The specificity of a test is defined as the proportion of patients who do not have the disease who will test negative for it. This can also be written as:

$$\text{specificity} = \frac{\text{number of true negatives}}{\text{number of true negatives} + \text{number of false positives}}$$

= probability of a negative test given that the patient is well
If a test has high specificity, a positive result from the test means a high probability of the presence of disease[13].

A false positive (with null hypothesis of health) in medicine causes unnecessary worry or treatment, while a false negative gives the patient the dangerous illusion of good health and the patient might not get an available treatment.

Accuracy = (True Positive + True Negative)/(True Positive + False Positive + False Negative + True Negative) [14,15]
Accuracy for cancerous nodule of size 10 mm template presented in segmented image

Image number	Specificity in %	Sensitivity in %	Accuracy
IMG-0003-00059.jpg	93.94	99.33	96.4793
IMG-0003-00060.jpg	93.90	99.40	96.4905
IMG-0003-00061.jpg	93.78	99.04	96.5714
IMG-0003-00062.jpg	93.83	99.19	96.3580
IMG-0003-00063.jpg	93.84	99.16	96.3520

Table 2: Sensitivity and specificity of nodule detection of radius 10 mm

Image number	Specificity in %	Sensitivity in %	accuracy
IMG-0003-00059.jpg	93.31	99.68	96.2735
IMG-0003-00060.jpg	93.60	99.70	96.4549
IMG-0003-00061.jpg	93.87	99.74	96.6183
IMG-0003-00062.jpg	93.12	99.63	96.1469
IMG-0003-00063.jpg	93.04	99.63	96.0982

Table 3: Rate of false positive providing accuracy of nodule detection of radius 15 mm

Image number	Specificity in %	Sensitivity in %	accuracy
IMG-0003-00059.jpg	93.29	99.69	96.2701
IMG-0003-00060.jpg	93.63	99.70	96.4655
IMG-0003-00061.jpg	93.86	99.74	96.6187
IMG-0003-00062.jpg	93.12	99.54	96.1112
IMG-0003-00063.jpg	93.02	99.62	96.0870

Table 4: Rate of false positive providing accuracy of nodule detection of radius 18 mm

Image number	Specificity in %	Sensitivity in %	accuracy
IMG-0003-00059.jpg	93.33	99.67	96.2817
IMG-0003-00060.jpg	93.59	99.71	96.4514
IMG-0001-00061.jpg	93.90	99.74	96.6392
IMG-0001-00062.jpg	93.14	99.62	96.1548
IMG-0010-00163.jpg	93.06	99.61	96.1069

Table 5: Rate of false positive providing accuracy of Jaupaxtral nodule detection of radius 18 mm Precision and accuracy curves for four nodules

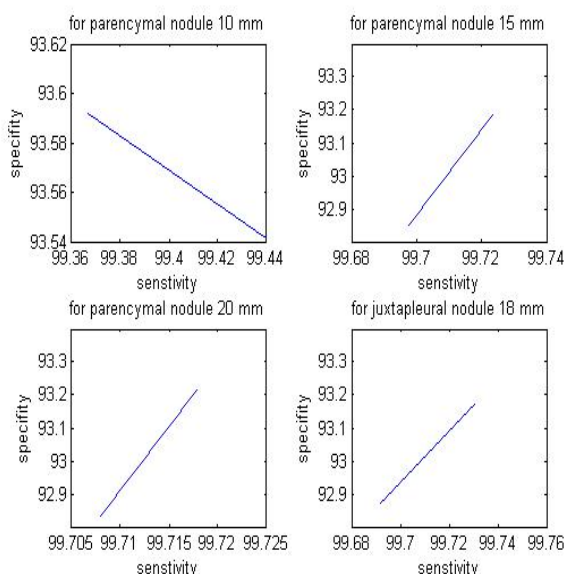


Fig 7: Graph tradeoff of sensitivity and specificity which result in final accuracy of 96 percent even though sensitivity of system is close to 99 percent which suggest the system is highly capable of detecting truly

VIII. CONCLUSION AND FUTURE WORK

An automated technique for the quantitative assessment of Lung Nodule Detection using LBP operators and template

matching has been developed. Rotation and scale invariant operators have been used to extract variance feature of image which is very efficient classifier when used in combination with linear binary patterns. These features capture the variation in the gray scale and rotation in images. Both nodule template and image to be diagnostic for abnormality has been converted in local binary pattern image and then the simple pattern matching algorithm has been implemented to extract nodules. The property included in images due to changing the images to local binary pattern enables process to identify nodule irrespective of in which orientation they are present. Due to small size of nodule and four rotation angles features selection the nodule has been classified with 100 percent accuracy and thus proved a good candidate for providing rotation invariant template for identification of nodule in image to be diagnosed for abnormality [16].

Future work will include applying model to three dimensional detection of nodule. A method for detection of solitary pulmonary nodule using LBB and template matching has shown very positive results with efficiency over 96 percent. The accuracy of the system can be further increased by increasing the size and quality of the template. It can also be increased by having more angles from 20°, to 10° or 5° in the texture class training set of nodule. The environmental conditions like, the reflection of the light influences the quality of the images and hence the efficiency of process.

REFERENCES

1. L. Ries et al. SEER Cancer Statistics Review 1973{1996. National Cancer Institution, Bethesda, MD, 1999.
2. Shodayu Takashima et al, "Indeterminate Solitary Pulmonary Nodules Revealed at Population-Based CT Screening of the Lung: Using First Follow-Up Diagnostic CT to Differentiate Benign and Malignant Lesions.," AJR 2003; 180:1255-1263
3. <http://www.radiologyassistant.nl/en/4609fcd50637>
4. P.R. Hill, D.R. Bull, C.N. Canagarajah, "Rotationally invariant texture features using the dual-tree complex wavelet transform", Proc. Int'l Conf. Image Process., vol. 3, IEEE, Vancouver, BC, Canada, 2000, pp. 901-904.
5. Edward H.S. Lo, Mark R. Pickering, Michael R. Frater, John F. Arnold, "Image segmentation from scale and rotation invariant texture features from the double dyadic dual-tree complex wavelet transform", © 2010 Elsevier, accepted 5 august 2010
6. Timo Ojala, Matti Pietikainen, Senior Member, IEEE, and Topi Maenpa suggested in 2002, "Multiresolution Gray-Scale and Rotation Invariant Texture Classification with Local Binary Patterns" July 2002
7. Zhenhua Guo, Lei Zhang, David Zhang, "Rotation invariant texture classification using LBP variance (LBPV) with global matching", Biometrics Research Centre, Department of Computing, The Hong Kong Polytechnic University, Hung Hom, Kowloon, Hong Kong, China, Pattern Recognition 43 (2010) 706-719
8. Timo Ojala, Matti Pietikainen, "Unsupervised texture segmentation using feature distributions", Machine Vision and Media Processing Group, Infotech Oulu, University of Oulu, FIN-90570 Oulu, Finland, Received 19 December 1997; in revised form 24 February 1998
9. <http://imaging.cancer.gov/programsandresources/informationssystemslide>
10. Timo Ojala, Matti Pietikainen Senior Member, IEEE, and Topi Maenpa, "Multiresolution Gray-Scale and Rotation Invariant Texture Classification with Local Binary Patterns", Pattern Recognition 49 (2010)
11. Hae Yong Kim, "Rotation-Discriminating Template Matching Based on Fourier Coefficients of Radial Projections with Robustness to Scaling and Partial Occlusion", Escola Politcnica, Universidade de São Paulo Av. Prof. Luciano Gualberto, tr. 3, 135, São Paulo, SP, 05508-010, Brazil.



Lung Image Segmentation Using Rotation Invariance and Template Matching

12. http://en.wikipedia.org/wiki/Sum_of_absolute_differences
13. <http://en.wikipedia.org/wiki/Cross-correlation>
14. en.wikipedia.org/wiki/Accuracy_and_precision
15. http://en.wikipedia.org/wiki/Sensitivity_and_specificity
16. Messay T, Hardie RC, Rogers SK, "Computationally efficient CAD system for pulmonary nodule detection in CT imagery", Med Image Anal. 2010 Jun;14(3):390-406. Epub 2010 Feb 19 (downloaded from: <http://www.ncbi.nlm.nih.gov/guide/>).